sciendo

ANNALS OF WEST UNIVERSITY OF
TIMISOARA PHYSICS

Vol. LXVI, 2024

DOI: 10.2478/awutp-2024-0013

# EFFECTS OF CROSSWINDS ON THE AEROTHERMAL BEHAVIOUR OF A DOUBLE-SKIN FAÇADE

Saber Ziari[1*], Rassim Belakroum[1], Saif Elislam Khelifa[2], Hocine Mansouri[2]

[1]*Univ. Ouargla, Fac. des Sciences Appliquées, Lab. Dynamique, Interaction et Réactivité des Systèmes, Ouargla 30000, Algeria,*
[2]*Univ. Ouargla, Fac. des Sciences Appliquées, Département de génie mécanique, Ouargla 30000, Algeria,*
[*]*Corresponding author: ziarisaber3@gmail.com*

| Article Info | Abstract |
|---|---|
| *Received: 11.03.2024*<br>*Accepted: 27.06.2024*<br><br>**Keywords:**<br>Double-skin facade, Passive ventilation, Unstable natural convection, Wind effect, Open vertical channel. | In double-skin facades, airflow is mainly induced by buoyancy forces due to temperature gradients and air compressibility. In practice, this passive system is also affected by ambient crosswind. The present work is focused on the analysis of the aerothermal behavior of an asymmetrically heated channel interacting with a transverse airflow. To achieve this, we utilized the computational fluid dynamics (CFD) technique based on the finite volume method to predict the system's performance. After validating the adopted numerical model, we examined the flow structure for different channel widths, and we determined the corresponding ventilation flow rates. We integrated the effect of wind with the thermosiphon effect. The thermo-aerodynamic performance of the facade was presented as a function of wind velocities, which significantly influence the airflow through the cavity and its openings. |

## 1. Introduction

The escalating global emphasis on sustainable development and energy transition underscores the critical role that energy efficiency in buildings must play in the broader context of climate change and environmental stewardship [1]. Notably, buildings are responsible for a significant proportion of global energy consumption and CO2 emissions, which necessitates the urgent implementation of effective strategies to enhance their energy performance. One such strategy is the use of double-skin facades (DSFs), a passive control system that can markedly enhance a building's thermal efficiency, acoustic isolation, and weather resistance [2].

The focus of this paper is on the aerothermal behavior of DSFs, specifically considering an asymmetrically heated channel in interaction with a transverse airflow. The airflow within DSFs is primarily driven by buoyancy forces generated by temperature differences and the compressibility of air. However, practical applications of DSFs also have to contend with external factors such as ambient crosswind, which can significantly affect the system's performance. Therefore, understanding the combined impact of these internal and external factors on a DSF's performance is crucial. This understanding can provide valuable insights for architects, engineers, and constructors aiming to design and develop more energy-efficient buildings, contributing to the larger goal of sustainable development [3].

The body of research on DSFs has grown significantly in recent years, with an array of studies exploring various aspects of these systems. For instance, some studies have delved into the potential benefits of integrating DSFs with other architectural and engineering systems. These include airflow networks, control logic for opening windows, and transparent photovoltaic modules [1]. Such integrations aim to enhance the energy efficiency of buildings, highlighting the versatile nature of DSFs and their potential for multifunctional applications.

Furthermore, recent research has also delved into the intersection of DSFs and digital technology, specifically the Internet of Things (IoT). Studies have investigated the potential impact of incorporating IoT technology into DSFs to optimize thermal comfort, a critical aspect of occupant well-being in buildings [4]. The integration of IoT within DSFs has the potential to revolutionize the design and operation of sustainable buildings. It signifies a paradigm shift in architectural design principles, marrying traditional design elements with cutting-edge digital technology.

In this study, we employ the computational fluid dynamics (CFD) technique to analyze and predict the system's performance. CFD, a reliable tool used for energy evaluation of glass facades [5], is based on the finite volume method. After validating the numerical model adopted in our study, we analyze the flow structure for different channel widths and determine the corresponding ventilation flow rates. We integrate the effect of wind with the thermosiphon effect and present the thermo-aerodynamic performance of the facade as a function of wind velocities.

This approach represents a significant contribution to the ongoing discourse on the energy efficiency of DSFs. It provides a comprehensive, nuanced analysis of the aerothermal behavior of an asymmetrically heated channel interacting with a transverse airflow. We anticipate that our findings will provide valuable insights for the design and implementation of DSFs in energy-efficient buildings. We hope to spur further research and innovation in this field, ultimately contributing to the global efforts to create a sustainable and resilient built environment.

Through the present work, we aim to investigate, using a numerical approach, the effect of winds on the performance of double skin facades and potentially solar chimneys. The approach used is purely numerical, employing the FLUENT code. This solver is based on the finite volume method and allows for solving problems of natural, mixed, or even forced convection.

## 2. Mathematical model

For the present study, the standard turbulence model $k-\varepsilon$ was used and the following assumptions were assumed to simplify the equations governing the studied phenomenon:

- The airflow was considered transient incompressible and two-dimensional.
- Heat transfer by radiation was not taken into account.
- The thermo-physical properties of the fluid are considered constant.
- Viscous dissipation was neglected.

The Boussinesq model was adopted. This model considers density as a constant value in all solved equations, except for evaluating the buoyancy term in the equation of the moment. In this case, we can write:

$$\rho-\rho_0=-\rho_0\ \beta(T-T_0)\,g \tag{1}$$

where: $\rho_0$ and $T_0$ are respectively the density and the ambient temperature. $\beta$ is the coefficient of thermal expansion.

The system of equations to be solved includes the continuity equation, the momentum equations, the energy equation and the kinetic energy transport equations $k$ and the dissipation rate $\varepsilon$. In this case, the system of equations to be solved in Cartesian coordinates takes the form:

i. Continuity equation

$$\frac{\partial\rho}{\partial t}+\frac{\partial(\rho U)}{\partial x}+\frac{\partial(\rho V)}{\partial y}=0 \tag{2}$$

ii. Quantity equations of movement

$$\frac{\partial u}{\partial t}+\frac{\partial (uu)}{\partial x}+\frac{\partial (vu)}{\partial x}=-\frac{1}{\rho}\frac{\partial P}{\partial x}+\frac{1}{\rho}\frac{\partial}{\partial x}\left[\mu_{eff}\frac{\partial u}{\partial x}\right]+\frac{1}{\rho}\frac{\partial}{\partial y}\left[\mu_{eff}\frac{\partial u}{\partial y}\right]-\frac{2}{3}\frac{\partial k}{\partial x} \quad (3)$$

$$\frac{\partial v}{\partial t}+\frac{\partial (uv)}{\partial x}+\frac{\partial (vv)}{\partial y}=-\frac{1}{\rho}\frac{\partial P}{\partial y}+\frac{1}{\rho}\frac{\partial}{\partial x}\left[\mu_{eff}\frac{\partial v}{\partial x}\right]+\frac{1}{\rho}\frac{\partial}{\partial y}\left[\mu_{eff}\frac{\partial v}{\partial y}\right]-\frac{2}{3}\frac{\partial k}{\partial x}+g\beta(T-T_0) \quad (4)$$

With:

$$\mu_{eff}=\mu+\mu_t$$

iii. Energy Equation

$$\frac{\partial T}{\partial t}+\frac{\partial (uT)}{\partial x}+\frac{\partial (vT)}{\partial y}=\frac{1}{\rho}\frac{\partial}{\partial x}\left[\left(\frac{\mu}{\Pr}+\frac{\mu_t}{\sigma_t}\right)\frac{\partial T}{\partial x}\right]+\frac{1}{\rho}\frac{\partial}{\partial y}\left[\left(\frac{\mu}{\Pr}+\frac{\mu_t}{\sigma_t}\right)\frac{\partial T}{\partial y}\right] \quad (5)$$

iv. Turbulent kinetic energy equation

$$\frac{\partial k}{\partial t}+\frac{\partial (uk)}{\partial x}+\frac{\partial (vk)}{\partial y}=\frac{1}{\rho}\frac{\partial}{\partial x}\left[\left(\mu+\frac{\mu_t}{\sigma_k}\right)\frac{\partial k}{\partial x}\right]+\frac{1}{\rho}\frac{\partial}{\partial y}\left[\left(\mu+\frac{\mu_t}{\sigma_k}\right)\frac{\partial k}{\partial y}\right]+\frac{1}{\rho}(G_k+G_b)-\varepsilon \quad (6)$$

Where the turbulent kinetic energy production terms $G_k$ and $G_b$ are calculated as follows:

$$G_k=\mu_t\left[\left(\frac{\partial u}{\partial y}+\frac{\partial v}{\partial x}\right)^2+2\left(\left(\frac{\partial u}{\partial x}\right)^2+\left(\frac{\partial v}{\partial y}\right)^2\right)\right]$$

$$G_b=\mu_t g\frac{\mu_t}{\sigma_t}\frac{\partial T}{\partial y}$$

In the above equations, $G_k$ represents the generation of turbulent kinetic energy due to the average velocity field gradient and $G_b$ is the turbulent kinetic energy induced by the effect of buoyancy.

v. Dissipation rate equation.

$$\frac{\partial \varepsilon}{\partial t}+\frac{\partial(u\varepsilon)}{\partial x}+\frac{\partial(v\varepsilon)}{\partial y}=\frac{1}{\rho}\frac{\partial}{\partial x}\left[\left(\mu+\frac{\mu_t}{\sigma_\varepsilon}\right)\frac{\partial \varepsilon}{\partial x}\right]+\frac{1}{\rho}\frac{\partial}{\partial y}\left[\left(\mu+\frac{\mu_t}{\sigma_\varepsilon}\right)\frac{\partial \varepsilon}{\partial y}\right]+C_{1\varepsilon}\frac{\varepsilon}{\rho k}\left(G_k+C_{3\varepsilon}G_b\right)-C_{2\varepsilon}\frac{\varepsilon^2}{k} \quad (7)$$

Where the turbulent (or swirling) viscosity, is calculated by combining $k$ and $\varepsilon$ as follows:

$$\mu_t=\rho C_\mu \frac{k^2}{\varepsilon} \quad (8)$$

For the $k-\varepsilon$ standard model, the $C_{1\varepsilon}, C_{2\varepsilon}, C_{3\varepsilon}, C_\mu, \sigma_t, \sigma_k$ and constants $\sigma_\varepsilon$ have the following values, 1.44, 1.92, 0.8, 0.09, 0.9, 1.0 and 1.3, respectively.

Turbulent flows are strongly affected by the presence of solids. Near-solid modeling has a significant impact on the fidelity of numerical solutions, as solids are the main source of vortex and medium turbulence. Therefore, the exact reproduction of the flow in the area close to the walls requires the use of the wall functions approach. These use semi-empirical formulas that provide an appropriate flow field in the area affected by the viscosity or boundary layer.

## 3. Numerical method

The solver of dynamics fluid problems FLUENT based on finite volume method was used in the present numerical investigations. The SIMPLE algorithm (acronym for Semi-Implicit Method for Pressure Linked Equations) is used to establish the coupling between the velocity and pressure fields ([6],[7]). The SIMPLE algorithm connects the momentum equations to the mass conservation equation using pressure corrections. The algorithm was chosen over others because of its robustness and efficiency in the computation of fluid flows.

## 4. Results and discussions

In order to be able to observe the effect of side winds on the aerothermal behavior of double-skinned facades, we must first validate the present numerical model by comparison with results available in the literature. It is necessary to explore the reference case without the presence of lateral air flow where the flow is due only to buoyancy forces. It is also important to note that we aim to analyze the effect of lateral ambient winds on the exit of the facade without disturbing the flow at the entrance. For this, we adopted the same strategy adopted by [6] in order to predict the effect of side winds on solar chimney power plants. All the results presented in this work correspond to a fully developed regime. The studied cases achieve the fully developed regime after approximately 60 seconds.

### 4.1. Validation and preliminary results

In order to ensure the veracity of the results obtained using the adopted numerical model, we have solved the case study previously treated by Lau et al. [8] concerning natural convection in an asymmetrically heated channel. Figure 1, illustrates the used calculation domain. Extended domains have been created at the upper and lower ends of the channel to suitably simulate the entrainment of ambient air near the inlet and outlet of the channel. The condition of adhesion to the walls is imposed on the solid walls. On the heated wall at x/W=0 and 0.186<y/H<1, a constant heat flux of 200 W/m² is applied as the boundary condition. We also imposed the pressure inlet conditions on borders 1,2,3,4 and 5, and the pressure outlet condition on 6,7,8,9, and 10. Figure 2, represents the variation of the air mass flow rate for a channel of dimensions H=1.956m and w=0.1m for different angles of inclination. Hence it is demonstrated that there is a good agreement between the results of this numerical investigation and that found by [8].

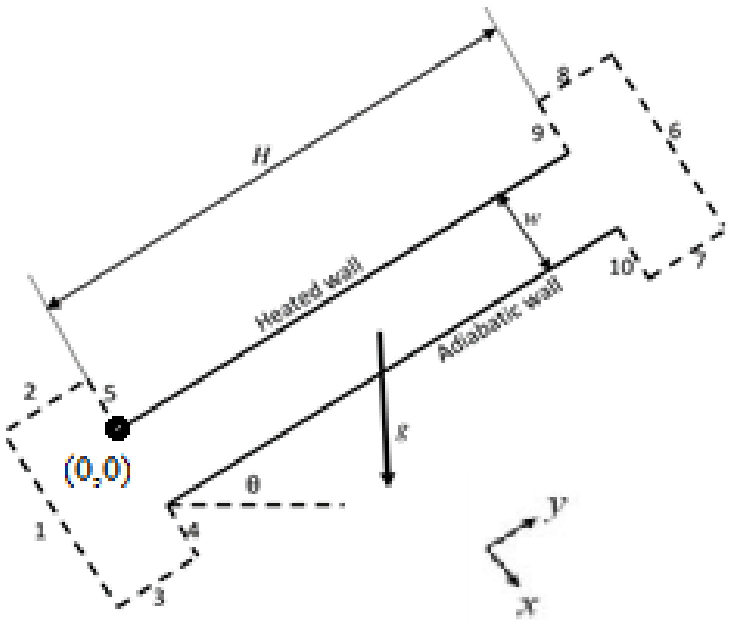


Figure 1. Geometry and area of calculation

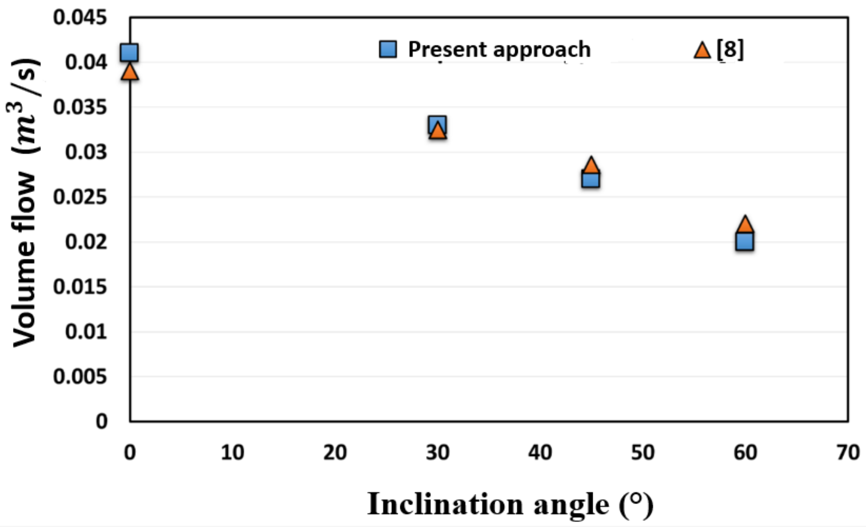


Figure 2. Volume flow rate for different inclination angles for a heat flow of 200W/m$^2$

**4.2. Effect of cavity width**

First, we have to invest the effect of increasing the width of a vertical double-skin facade B on the air flow, particularly at the outlet. In the first place we will consider the thermosiphon effect. The phenomenon of cooler external fluid entering through the outlet of the chimney has been reported by several researchers who have reported the appearance of a reverse flow at the outlet of the chimney that penetrated deeper into the chimney with the increase in the width of the channel [8]. The results of our simulations perfectly reflect this phenomenon. From Figure 3, it is noted that for B=0.5m, there is no fluid inlet through the outlet of the channel, on the other hand for B=0.6m a reverse flow zone has formed close to the adiabatic wall. This area grows larger and its size increases even more for B=0.75m. When the width B=1m, the appearance of a second recirculation zone is observed and according to the structure of the flow, two distinct zones can be identified in this case, one with the positive speed (upward) and the other with the negative speed (downward). These are associated with the reverse flow entering from the output. The appearance of a reverse flow at the outlet of the chimney is the cause of the reduction in mass flow to the increase in the width of the channel as reported by [9].

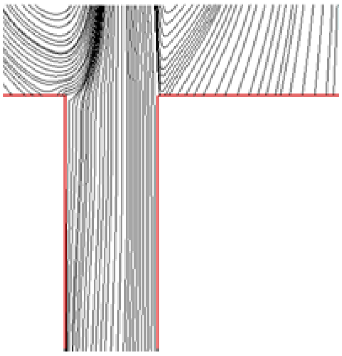

(a) B=0.5m

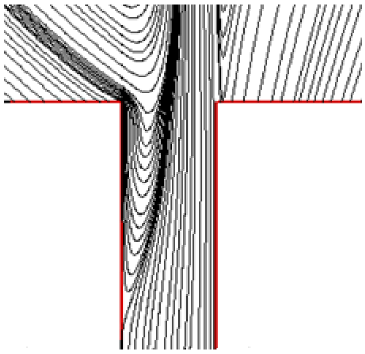

(b) B=0.6m

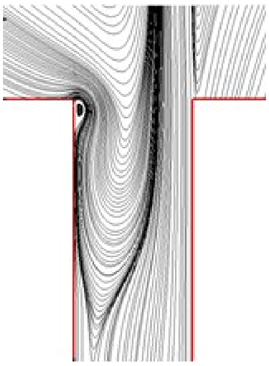

(c) B=0.75m

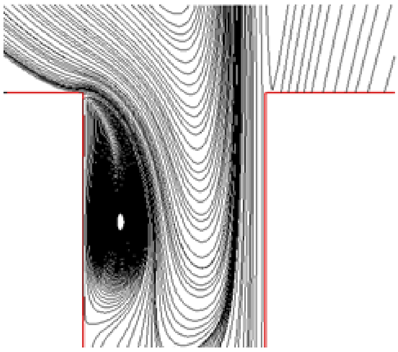

(d) B=1m

Figure 3. Streamlines for different widths and heat flux of 600 W/m$^2$

Figure 4 shows that the predicted ventilation volume flow rate increases with the heat flux at the absorber. The volume flow also increases with channel width from 0.25m to 0.5m, then decreases as the width increases between 0.5m and 1m. From Figure 5, representing the velocity profiles at the outlet of the channel, it can be seen that the airflow is ascending over the entire width for b= 0.5m. However, for larger widths i.e. 0.6, 0.75 and 1m, an ascending airflow is observed near the absorber due to buoyancy forces, but near the adiabatic wall, the air flows from top to bottom.

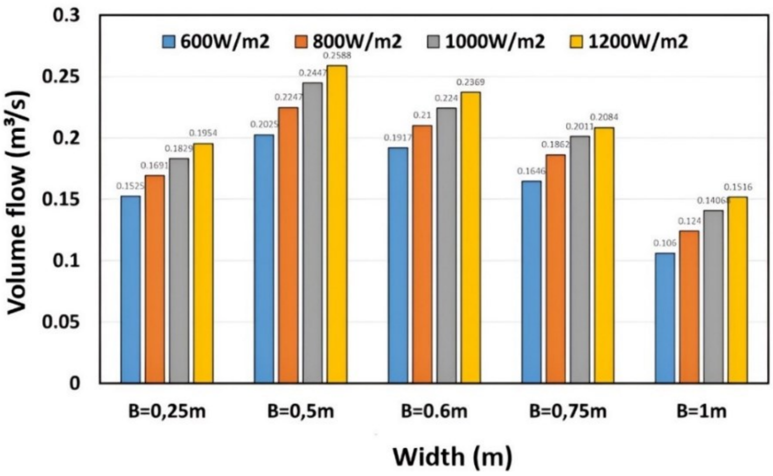


Figure 4. Variation in volume flow as a function of cavity width for different heat flux

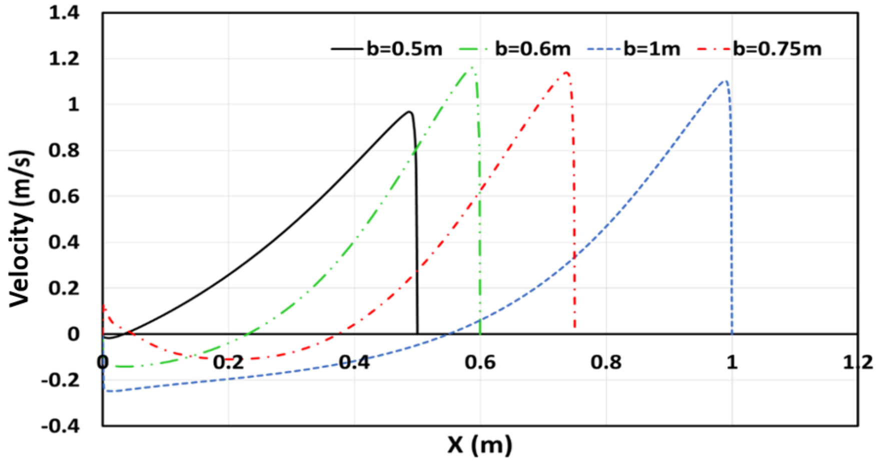


Figure 5. Channel outlet velocity profile for different widths for heat flux $\phi$=600W/m$^2$ (x=0 corresponds to the adiabatic wall)

The effect of chimney width on heat transfer within the studied channel is evidenced by the mean Nusselt number curves calculated on the absorber, as shown in Figure 6. This graph indicates that the heat transfer rate decreases with increasing width of the facade

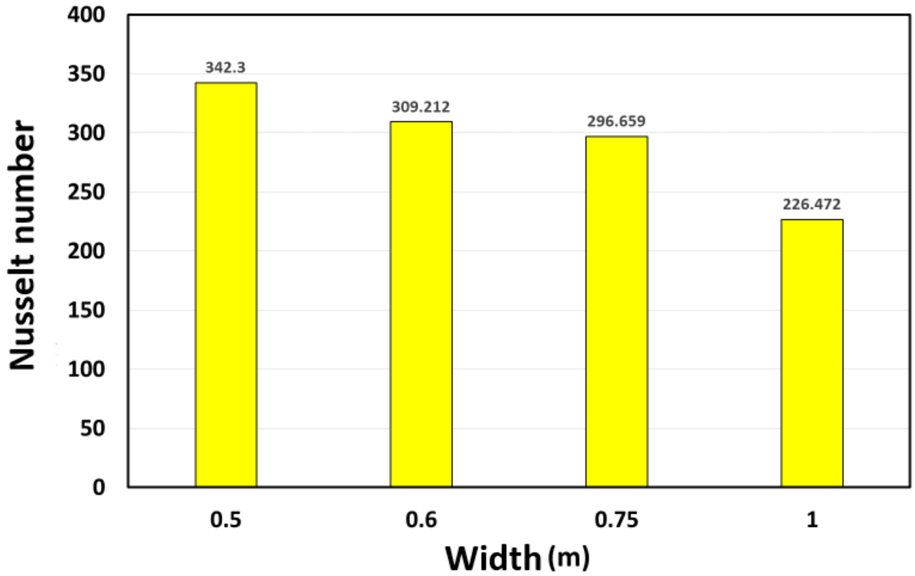


Figure 6. Variation of the average Nusselt number at the absorber as a function of the width of the cavity

### 4.3. Crosswind effect

Figure 7 depicts the calculation domain used and the imposed boundary conditions. It displays the inner domain of the asymmetrically heated channel and its surrounding vicinity. Essentially, the study involves simulating the turbulent flow of an incompressible fluid inside and around an asymmetrically heated vertical channel. The airflow consists of warm air interacting with cross airflow.

The airflow in a double skin facade is of the elliptical type, i.e. the flow inside the channel depends on the flow beyond its outlet. If the flow around the outlet of the vertical channel is changed this will also affect the structure of the airflow in the facade. As shown in Figure 8, in the absence of side winds, the flow beyond the outlet is structured into two large vortex structures that evolve slowly over time without too much affecting the flow inside the channel and therefore, the calculation domain could be limited to the vertical channel with a pressure outlet type outlet condition. The results in this case are considered acceptable.

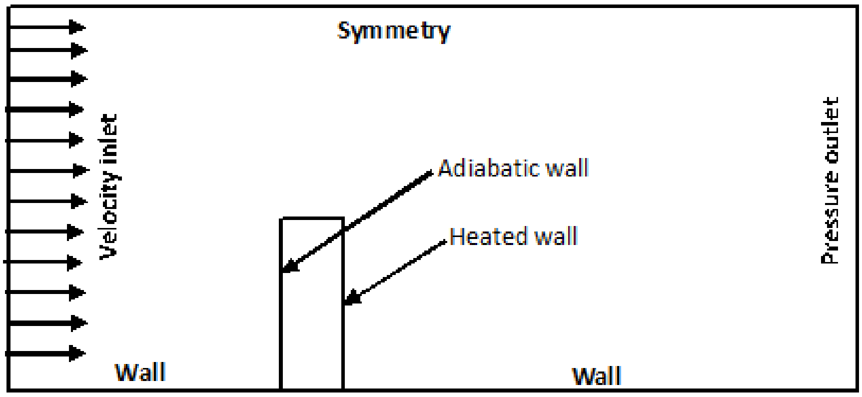


Figure 7. Calculation domain and boundary conditions

According to Figure 9, the presence of a side wind from 0.5m/s categorically modifies the topology of the flow around and inside the double-skin facade. At the outlet of the channel, the recirculation zones that existed near the adiabatic wall disappear and give rise to a recirculation zone in the middle of the channel near its outlet. From 1m/s, the vortices that hindered the flow inside the vertical channel disappear because they are sucked out. This is mainly caused by the negative pressure areas at the outlet of the channel that have been formed by the effect of side winds.

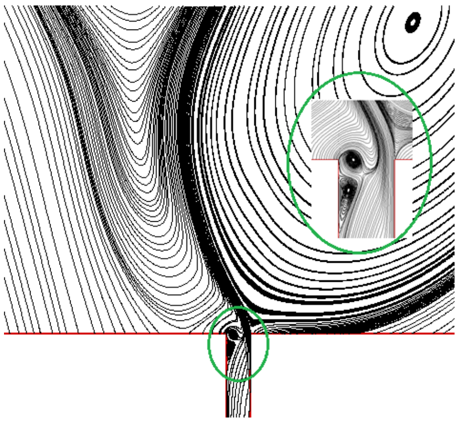

Figure 8. Streamlines for B=1m, and heat flux of $\phi$=600W/m$^2$ without crosswind effects

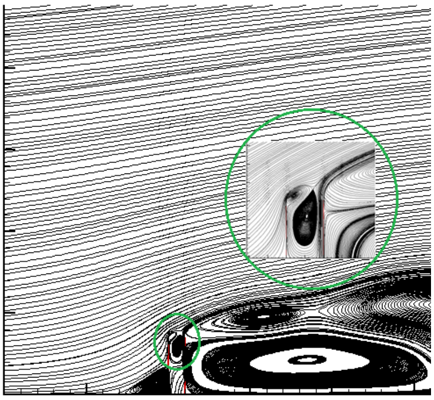

**(a)** V=0.5m/s

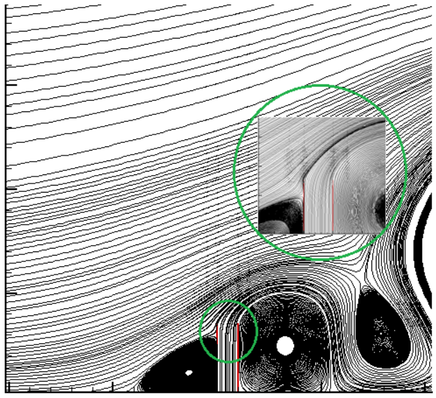

**(b)** V=1m/s

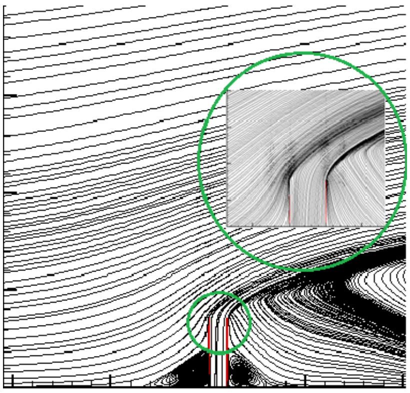

**(c)** V=2m/s

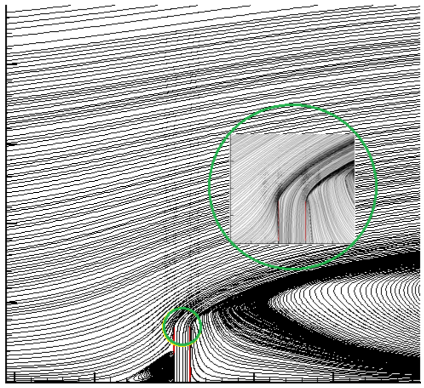

**(d)** V=3m/s

Figure 9. Streamlines for B=1m, heat flow $\phi$=600W/m$^2$ and in the presence of crosswinds

Figure 10, shows the velocity profiles at the exit of the 1m wide double-skin facade for different wind velocities. The positive effect of crosswinds is highlighted. We notice the increase in velocities according to the wind velocity. It is also noted that the effect is not symmetrical as it depends on the direction of the atmospheric air flow.

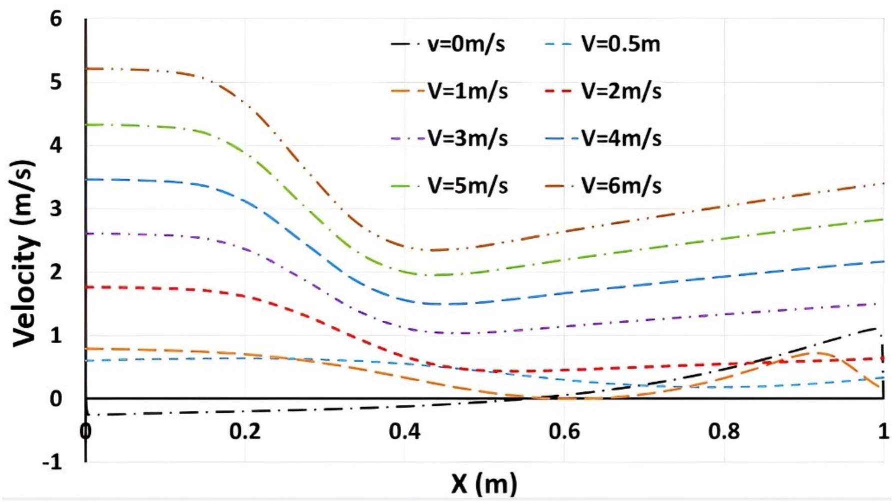


Figure 10. Outlet velocity profile for B=1m, heat flux $\phi$=600W/m$^2$ and different crosswind velocities

For a double-skin facade, the ventilation flow rate is the most important parameter. In reality, we are looking for anything that improves the ventilation capabilities of the system in question. Figure 11 shows the variation of the volume flow as a function of the lateral wind velocity for two widths B=0.5m and 1m. According to our results, in the absence of crosswind, the ventilation rate provided by a 0.5m wide facade is almost double that of a 1m wide façade. This result can be also observed in Figure 4. Nevertheless, during the existence of a lateral atmospheric flow at 0.5m/s the behavior reverses because the ventilation flow of the facade at 1m width exceeds by 25% that of 0.5m. From Figure 11, it is evident that the volume flow rate increases with increasing wind velocity. It is also noted that the effect of the wind is greater on the facade of 1m width compared to that of 0.5m especially for wind velocities greater than 5m/s.

The effect of chimney width on heat transfer within the studied channel is evidenced by the mean Nusselt number curves calculated on the absorber, as shown in Figure 12. This graph indicates that the heat transfer rate increases with increasing crosswind velocity.

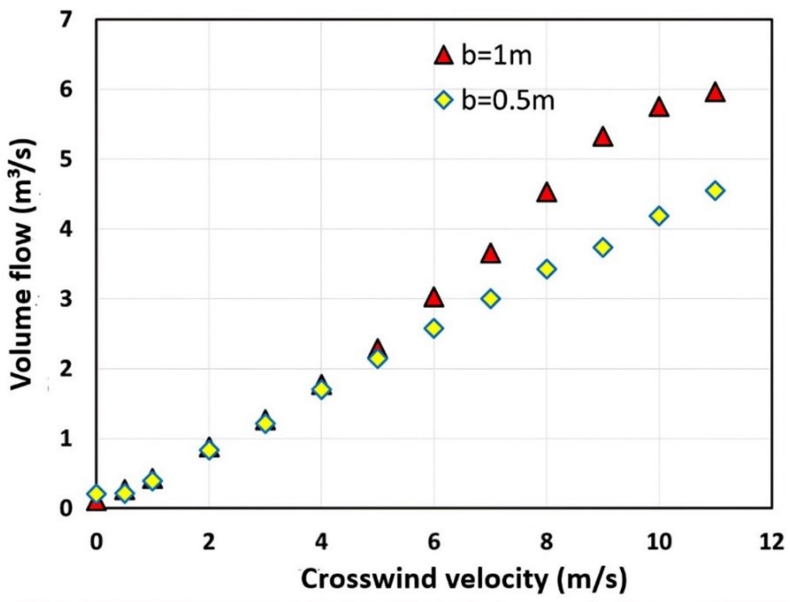


Figure 11. Variation in volume flow as a function of crosswind velocity

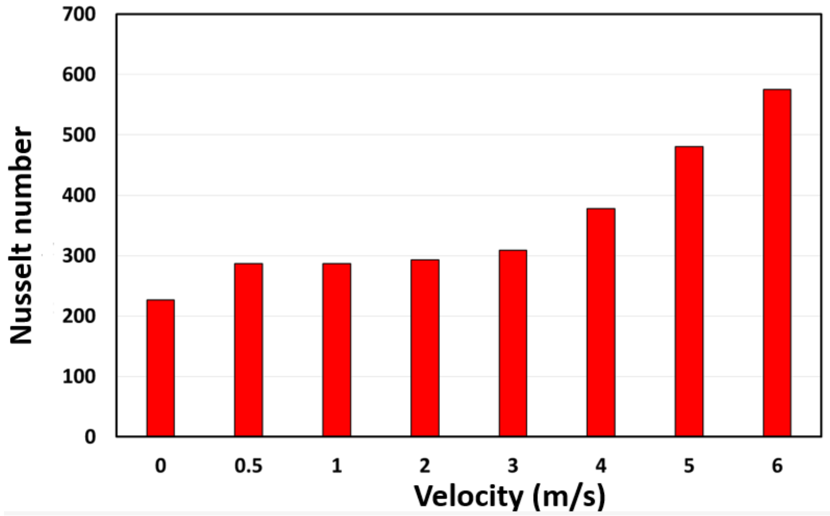


Figure 12. Variation in the average Nusselt number at the absorber as a function of wind speed for B=1m

## 5. Conclusions

In conclusion, the study has revealed the substantial impact of lateral winds on the aerothermal behavior of upward airflow solar systems, particularly double skin facades. With numerical simulations, key findings include an increase in the ventilation rate corresponding with the heat flux at the absorber, the emergence of reverse flows at the exit increasing with the channel width, and changes in the heat transfer rate in relation to the width of the facade and speed of lateral winds. These results highlight the necessity to account for wind effects in the development of passive solar systems. Despite the comprehensive analysis, the study acknowledges the limitations inherent in using numerical simulations, which may not fully replicate real-world complexities. The findings shed light on the sophisticated dynamics of passive solar systems under the influence of lateral winds, paving the way for future research. Further exploration could examine other environmental factors, or employ different simulation methods to verify and build upon our findings, thereby advancing the design and efficiency of these sustainable systems.

## References

[1] F. Ascione, N. Bianco, F. de Rossi, F. Iovne, and G. M. Mauro, *Are transparent double-skin facades effective for energy retrofit? Answers for an office building-with and without photovoltaic integration*, Energy Sources, Part A: Recovery, Utilization, and Environmental Effects, 44.1 (2022) 257-271.

[2] A. Sofi, and F. Genovese, *Stochastic analysis of double-skin façades subjected to imprecise seismic excitation*, Materials Research Proceedings, 26 (2023) 555-560.

[3] B. Charles, F. Bode, and C. Croitoru, *Numerical simulation investigation of a double skin transpired solar air collector*, Applied Sciences, 12.1 (2022) 520.

[4] A. M. Khorasgani,N. Zare, and A. Rodriguez, *Using IoT in Double Skin Facades toward Thermal Comfort: A Review*, Urban Planning and Construction, 2.1 (2024) 1-10.

[5] M. Bugarin, S. Nizetic, M. Bugarin, B. Bralic, and M. Omazic, *Innovative approaches in energy efficiency evaluation of glazed facades in nZEB buildings*, 7th International Conference on Smart and Sustainable Technologies (SpliTech). IEEE, (2022) 1-5.

[6] W. Shen, T. Ming, Y. Ding, Y. Wu, and R.K. de_Richter, *Numerical analysis on an industrial-scaled solar updraft power plant system with ambient crosswind*, Renewable energy, 68 (2014) 662-676.

[7] T. Ming, Y. Wu, R. K. de_Richter, W. Liu, and S. A. Sherif, *Solar updraft power plant system: A brief review and a case study on a new system with radial partition walls in its collector*, Renewable and Sustainable Energy Reviews, 69 (2017) 472-487.

[8] G. E. Lau, V. Timoshenko, J. Reizes, M. Fossa, and G. H. Yeoh, *Natural convection in an asymmetrically-heated open-ended channel: a three-dimensional computational study*, Heat Transfer Summer Conference. American Society of Mechanical Engineers, 55492 (2013).

[9] G. Gan, and S. B. Riffat, *A numerical study of solar chimney for natural ventilation of buildings with heat recovery,* Applied Thermal Engineering, 18.12 (1998) 1171-1187.